Vibration and buckling analyses of nanobeams embedded in an elastic medium

S Chakraverty† and Laxmi Behera

Department of Mathematics, National Institute of Technology Rourkela, Odisha, India

(Received 14 February 2015; revised manuscript received 23 April 2015; published online 3 August 2015)

Boundary characteristic orthogonal polynomials are used as shape functions in the Rayleigh–Ritz method to investigate vibration and buckling of nanobeams embedded in an elastic medium. The present formulation is based on the nonlocal Euler–Bernoulli beam theory. The eigen value equation is developed for the buckling and vibration analyses. The orthogonal property of these polynomials makes the computation easier with less computational effort. It is observed that the frequency and critical buckling load parameters are dependent on the temperature, elastic medium, small scale coefficient, and length-to-diameter ratio. These observations are useful in the mechanical design of devices that use carbon nanotubes.

Keywords: Rayleigh–Ritz method, boundary characteristic orthogonal polynomials, nonlocal elasticity theory, Euler–Bernoulli beam theory

PACS: 73.63.Fg, 65.80.–g, 66.70.Lm, 02.60.–x **DOI:** 10.1088/1674-1056/24/9/097305

1. Introduction

Recently, nanomaterials have aroused interest among the scientific communities in the fields of physics, chemistry, and engineering. Some of these materials are nanoparticles, nanowires,[1–4] nanotubes,[5–15] and nanotube resonators. Among them, beam type structures play a vital role in the field of nanotechnology. The discovery of carbon nanotubes by Ijima[16] has sparked a revolution in nanotechnology. Because of the unique characteristics of carbon nanotubes,[17] they have been recognized as promising materials for future applications such as nanodevices, nanocomposites, and nanoelectronics. Conducting experiments at nanoscale size is quite difficult. Molecular dynamics is one of the effective ways to study the mechanical properties of nanostructures. But the molecular dynamics simulation is time consuming and arduous for large-scaled CNTs. Accordingly, classical continuum mechanics is being increasingly viewed as an efficient way to study nanostructured materials. But these continuum models do not capture small scale effects. Hence various nonlocal continuum theories have been proposed to study mechanical behaviors of structures at nanoscale. One of the nonlocal continuum theories is the nonlocal elasticity theory pioneered by Eringen.[18] Beam and shell models have been developed based on the nonlocal elasticity theory to model nanostructures. Peddieson *et al.*[19] applied the nonlocal continuum model to nanotechnology. Xu[20] found that the nonlocal effect has significant influences on the natural frequency and vibration modes in nanostructures. Since conducting experiments at nanoscale size is quite difficult, development of mathematical models is necessary. Hence analytical and numerical methods have been developed by the authors to investigate static and dynamic problems of nanobeams.[21–26] Study of various aspects of nanotubes such as buckling, mechanical, chemical, and thermal properties attracts tremendous attention of researchers. Thermal effects are significant in vibration and buckling analyses since the increase in temperature leads to the increase in carbon–carbon (C–C) bond length in the CNTs, which induces an axial and radial force within CNTs. Thermal vibration frequencies may be used to estimate Young's modulus of various nanotubes.[27] Therefore, the investigation of the thermal effect on the mechanical properties of CNTs is very important. Moreover, the surrounding elastic medium has a great influence on the frequencies and buckling loads of carbon nanotubes. Some researchers have considered the thermal effect in the vibration and buckling analyses of nanotubes. A few of them are cited below.

Free vibration of single-walled carbon nanotubes (SWCNTs) has been investigated based on the nonlocal Levinson beam theory[27] and the Timoshenko beam theory[28,29] in a thermal environment. The authors found that vibration characteristics are strongly dependent on the temperature change. Similar thermal effect may also be seen when one analyzes the instability of SWCNTs conveying fluid.[30] The thermal effect on the vibration of double-walled carbon nanotubes has been investigated analytically by Zhang *et al.*[31] for simply supported edge condition. The differential quadrature method has been employed by Murmu and Pradhan[32] to study thermo mechanical vibration of SWCNTs embedded in an elastic medium. The authors applied the same method for buckling analysis of SWCNTs embedded in an elastic medium[33] based on the nonlocal Timoshenko beam theory. Buckling analysis of SWCNTs embedded in an elastic medium has also been presented analytically by Narendar and Gopalakrishnan[34] in a

†Corresponding author. E-mail: snechak@gmail.com

© 2015 Chinese Physical Society and IOP Publishing Ltd

thermal environment. Thermal buckling analysis of embedded SWCNTs has also been investigated in Refs. [35] and [36]. Tounsi *et al.*[37] analyzed buckling behavior of nanobeams based on the higher order beam theory.

Recently, efforts have been made by the researchers to develop efficient numerical and analytical methods for obtaining desired results with ease. Numerical methods such as differential quadrature and finite element have been applied with simple boundary conditions such as simply supported. However, it is sometimes tedious to apply such numerical methods in the complicated problems for all sets of boundary conditions. In this context, one may use the Rayleigh–Ritz method (R–R), which is quite easy to handle for all classical boundary conditions. Previously, authors have applied boundary characteristic orthogonal polynomials as shape functions in the R–R method to analyze static and dynamic problems of beam or plate elements.[38–43] However, to the best of our knowledge, this is the first attempt on the application of the R–R method for the vibration and buckling analysis of nanobeams embedded in an elastic medium under the influence of temperature. In this article, boundary characteristic polynomials are implemented in the R–R method. The use of boundary characteristic polynomials in the R–R method produces results with high accuracy, stable computation, and rapid convergence. Because of the orthogonal property of boundary characteristic polynomials, some of the entries of stiffness and mass matrices become either zero or one. Effects of the surrounding elastic medium, temperature, nonlocal parameter, and length-to-diameter ratio on the frequency and critical buckling load parameters are systematically analyzed.

2. Problem formulation

This study is carried out on the basis of the Euler–Bernoulli beam theory in conjunction with the nonlocal elasticity theory of Eringen.[18] For applying the present method, one needs to have knowledge about energies. Therefore, at first we have given an overview of the energies of nanobeams based on the Euler–Bernoulli beam theory. Here the x coordinate is taken along the length of the beam and the z coordinate is measured from the mid-plane of the beam.

2.1. Euler–Bernoulli beam theory

The strain energy U may be written as

$$U = \frac{1}{2}\int_0^L \int_A \sigma_{xx}\varepsilon_{xx}\,\mathrm{d}A\,\mathrm{d}x, \tag{1}$$

where σ_{xx} is the normal stress, L is the length of the beam, and A is the cross-section area. Here normal strain ε_{xx} is given by the following relationship:

$$\varepsilon_{xx} = -z\frac{\partial^2 w}{\partial x^2}, \tag{2}$$

where w is the deflection function. Substituting Eq. (2) in Eq. (1), we obtain

$$U = -\frac{1}{2}\int_0^L M\frac{\partial^2 w}{\partial x^2}\,\mathrm{d}x, \tag{3}$$

where M is the bending moment and is defined as $M = \int_A z\sigma_{xx}\,\mathrm{d}A$. Assuming free harmonic motion, i.e., $w = w_0(x)\sin\omega t$, where ω is the natural frequency of vibration, one may obtain strain energy U as

$$U = -\frac{1}{2}\int_0^L M\frac{\mathrm{d}^2 w_0}{\mathrm{d}x^2}\,\mathrm{d}x. \tag{4}$$

The kinetic energy is given as

$$T = \frac{1}{2}\int_0^L \rho A\omega^2 w_0^2\,\mathrm{d}x, \tag{5}$$

where ρ is the mass density of beams.

The potential energy (the work done by external forces) may be given as[44]

$$V = \frac{1}{2}\int_0^L \left[\bar{N}\left(\frac{\mathrm{d}w_0}{\mathrm{d}x}\right)^2 + f_e w_0\right]\mathrm{d}x, \tag{6}$$

where $\bar{N}$ is the applied compressive force and is expressed as $\bar{N} = N_\mathrm{m} + N_\theta$. Here N_m is the axial force due to the mechanical loading prior to buckling, and N_θ is the axial force due to the influence of the temperature change, $N_\theta = -EA\alpha_x\theta/(1-2\nu)$, where E is the Young's modulus, A is the cross-section area, ν is the Poisson's ratio, α_x is the coefficient of thermal expansion in the x direction, and θ is the change in temperature. The f_e is the density of reaction force of elastic foundation which is expressed as $f_e = k_w w_0 - k_g\,\mathrm{d}^2 w_0/\mathrm{d}x^2$. Here k_w denotes the Winkler modulus and k_g denotes the shear modulus of the elastic medium.

Using Hamilton's principle

$$\int_0^t \delta T - (\delta U + \delta V)\,\mathrm{d}t = 0 \tag{7}$$

and setting the coefficient of δw_0 to zero, we obtain the following governing equation of motion:

$$\frac{\mathrm{d}^2 M}{\mathrm{d}x^2} + \bar{N}\frac{\mathrm{d}^2 w_0}{\mathrm{d}x^2} - k_w w_0 + k_g\frac{\mathrm{d}^2 w_0}{\mathrm{d}x^2} = -\rho A\omega^2 w_0. \tag{8}$$

Based on Eringen's nonlocal elasticity theory, the nonlocal constitutive equation of EBT nanobeam is given by[23]

$$M - \mu\frac{\mathrm{d}^2 M}{\mathrm{d}x^2} = -EI\frac{\mathrm{d}^2 w_0}{\mathrm{d}x^2}, \tag{9}$$

where $\mu = (e_0 a)^2$ is the nonlocal parameter and I is the second moment of area. By using Eqs. (8) and (9), M in nonlocal form may be written as

$$M = -EI\frac{\mathrm{d}^2 w_0}{\mathrm{d}x^2} + \mu\left(-\rho A\omega^2 w_0 - \bar{N}\frac{\mathrm{d}^2 w_0}{\mathrm{d}x^2}\right.$$

$$+k_{\mathrm{w}}w_0-k_{\mathrm{g}}\frac{\mathrm{d}^2w_0}{\mathrm{d}x^2}\Bigg).$$

For simplicity and convenience in mathematical formulation, the following non-dimensional parameters have been used:

$$X=\frac{x}{L},\ W=\frac{w_0}{L},\ \beta=\frac{e_0a}{L},$$
$$\hat{N}=\frac{\bar{N}L^2}{EI},\ \lambda^2=\frac{\rho A\omega^2L^4}{EI},\ K_{\mathrm{g}}=\frac{k_{\mathrm{g}}L^2}{EI},$$
$$K_{\mathrm{w}}=\frac{k_{\mathrm{w}}L^4}{EI},\ \hat{N}_\theta=\frac{N_\theta L^2}{EI},\ \hat{N}_{\mathrm{m}}=\frac{N_{\mathrm{m}}L^2}{EI}.$$

Equating maximum kinetic and potential energies, one may obtain the following expressions for EBT nanobeams:

$$\begin{aligned}&\rho A\omega^2L^2\left[W^2-\beta^2W\frac{\mathrm{d}^2W}{\mathrm{d}X^2}\right]\\&=\frac{EI}{L^2}\left[\left(\frac{\mathrm{d}^2W}{\mathrm{d}X^2}\right)^2+\hat{N}\beta^2\left(\frac{\mathrm{d}^2W}{\mathrm{d}X^2}\right)^2-K_{\mathrm{w}}\beta^2W\frac{\mathrm{d}^2W}{\mathrm{d}X^2}\right.\\&+K_{\mathrm{g}}\beta^2\left(\frac{\mathrm{d}^2W}{\mathrm{d}X^2}\right)^2+\hat{N}\left(\frac{\mathrm{d}W}{\mathrm{d}X}\right)^2\\&\left.+K_{\mathrm{w}}W^2-K_{\mathrm{g}}W\frac{\mathrm{d}^2W}{\mathrm{d}X^2}\right].\end{aligned}\tag{10}$$

2.2. Solution procedure

For applying the R–R method, unknown function W may be written in a series of simple polynomials ($X^{i-1}, i=1,2,\ldots,n$) multiplied by a boundary function which ensures that the unknown function satisfies the essential geometric boundary conditions of the beam. The displacement may be expressed as

$$W(X)=\sum_{k=1}^{N}c_k\hat{\phi}_k,\tag{11}$$

where N is the number of terms required to compute results, c_k are unknowns, and $\hat{\phi}_k$ are orthonormal polynomials that are obtained by using the Gram–Schmidt process. The orthogonal polynomials have been generated over the region $0\le X\le 1$ with the help of a linearly independent set of functions $\delta_k=ll_k$, $k=1,2,3,\ldots,N$, with $l=X^m(1-X)^n$ and $l_k=X^{k-1}$. The m takes the values $0,1,2$ accordingly as the edge $X=0$ is free, simply supported, or clamped. The same justification can be given to n for the edge $X=1$. The orthonormal polynomials have been generated by the following steps:

$$\phi_1=\delta_1,\ \ \phi_k=\delta_k-\sum_{j=1}^{k-1}\psi_{kj}\phi_j,\tag{12}$$

where

$$\psi_{kj}=\frac{\langle\delta_k,\phi_j\rangle}{\langle\phi_j,\phi_j\rangle},\quad k=2,3,\ldots,N,$$
$$j=1,2,\ldots,k-1.$$

Here $\langle\,\rangle$ denotes the inner product of two functions and we define the inner product of two functions, say ϕ_i and ϕ_k, as

$$\langle\phi_i,\phi_k\rangle=\int_0^1\phi_i(X)\phi_k(X)\mathrm{d}X.\tag{13}$$

Similarly, the norm of the function ϕ_i may be defined as

$$\|\phi_i\|=\int_0^1\phi_i^2(X)\mathrm{d}X.$$

Then normalized function ϕ_i may be obtained by using

$$\hat{\phi}_i=\frac{\phi_i}{\|\phi_i\|}.$$

It should be noted that using the boundary characteristic orthogonal polynomial series as the admissible functions has distinct advantages since they are a set of orthogonal series. Therefore, more rapid convergence and better stability in the numerical computation may be achieved.

Free vibration analysis In the case of free vibration, one may obtain the Rayleigh quotient from the following equation of EBT nanobeams:

$$\begin{aligned}&\lambda^2\left[W^2-\beta^2W\frac{\mathrm{d}^2W}{\mathrm{d}X^2}\right]\\&=\left(\frac{\mathrm{d}^2W}{\mathrm{d}X^2}\right)^2+\hat{N}_\theta\beta^2\left(\frac{\mathrm{d}^2W}{\mathrm{d}X^2}\right)^2-K_{\mathrm{w}}\beta^2W\frac{\mathrm{d}^2W}{\mathrm{d}X^2}\\&+K_{\mathrm{g}}\beta^2\left(\frac{\mathrm{d}^2W}{\mathrm{d}X^2}\right)^2+\hat{N}_\theta\left(\frac{\mathrm{d}^2W}{\mathrm{d}X^2}\right)^2\\&+K_{\mathrm{w}}W^2-K_{\mathrm{g}}W\frac{\mathrm{d}^2W}{\mathrm{d}X^2}.\end{aligned}\tag{14}$$

It may be noted here that we have to take $\hat{N}_{\mathrm{m}}=0$ in Eq. (10).

Buckling analysis For the buckling analysis, the following eigen equation for EBT nanobeams may be derived from Eq. (14) by setting the inertia term to zero and $\hat{N}_{\mathrm{m}}=-P$:

$$\begin{aligned}&\hat{P}\left[\left(\frac{\mathrm{d}W}{\mathrm{d}X}\right)^2+\beta^2\left(\frac{\mathrm{d}^2W}{\mathrm{d}X^2}\right)^2\right]\\&=\left(\frac{\mathrm{d}^2W}{\mathrm{d}X^2}\right)^2-K_{\mathrm{w}}\beta^2W\frac{\mathrm{d}^2W}{\mathrm{d}X^2}+K_{\mathrm{g}}\beta^2\left(\frac{\mathrm{d}^2W}{\mathrm{d}X^2}\right)^2\\&+K_{\mathrm{w}}W^2-K_{\mathrm{g}}W\frac{\mathrm{d}^2W}{\mathrm{d}X^2}+\frac{\hat{N}_\theta L^2}{EI}\left(\frac{\mathrm{d}^2W}{\mathrm{d}X^2}\right)^2\\&+\frac{N_\theta L^2}{EI}\beta^2\left(\frac{\mathrm{d}^2W}{\mathrm{d}X^2}\right)^2,\end{aligned}\tag{15}$$

where $\hat{P}=PL^2/(EI)$.

Substituting Eq. (11) in Eq. (14) and minimizing λ^2 with respect to the coefficients of the admissible functions that is $\partial\lambda^2/\partial c_j=0$, one may obtain the following eigenvalue value problem:

$$[\boldsymbol{K}]\{\boldsymbol{Y}\}=\lambda^2[\boldsymbol{M}]\{\boldsymbol{Y}\},\tag{16}$$

where $\boldsymbol{Y}=\{c_1\ c_2\ \cdots\ c_N\}^{\mathrm{T}}$, stiffness matrix $\boldsymbol{K}$ and mass matrix $\boldsymbol{M}$ are given by

$$K(i,j)=\int_0^1(2\phi_i''\phi_j''+2\hat{N}\beta^2\phi_i''\phi_j''-K_{\mathrm{w}}\beta^2\phi_i''\phi_j$$

$$
\begin{aligned}
&- K_{\mathrm{w}}\beta^2\phi_i\phi_j'' + 2K_{\mathrm{g}}\beta^2\phi_i''\phi_j'' + 2\hat{N}\phi_i'\phi_j' \\
&+ 2K_{\mathrm{w}}\phi_i\phi_j - K_{\mathrm{g}}\phi_i''\phi_j - K_{\mathrm{g}}\phi_i\phi_j'')\,\mathrm{d}X, \\
M(i,j) &= \int_0^1 (2\phi_i\phi_j - \beta^2\phi_i''\phi_j - \beta^2\phi_i\phi_j'')\,\mathrm{d}X.
\end{aligned}
$$

Similarly, substituting Eq. (11) in Eq. (15) and minimizing $\hat{P}$ with respect to the coefficients of the admissible functions, that is $\partial\hat{P}/\partial c_j = 0$, the following eigenvalue value problem may be obtained:

$$
[\boldsymbol{K}]\{\boldsymbol{Z}\} = \hat{P}[\boldsymbol{B}]\{\boldsymbol{Z}\}, \tag{17}
$$

where $\boldsymbol{Z} = \{c_1\ c_2\ \cdots\ c_N\}^{\mathrm{T}}$, stiffness matrix $\boldsymbol{K}$ and buckling matrix $\boldsymbol{B}$ are given by

$$
\begin{aligned}
K(i,j) &= \int_0^1 (2\phi_i''\phi_j'' - K_{\mathrm{w}}\beta^2\phi_i''\phi_j - K_{\mathrm{w}}\beta^2\phi_i\phi_j'' \\
&+ 2K_{\mathrm{g}}\beta^2\phi_i''\phi_j'' + 2K_{\mathrm{w}}\phi_i\phi_j - K_{\mathrm{g}}\phi_i''\phi_j - K_{\mathrm{g}}\phi_i\phi_j'' \\
&+ 2\hat{N}\beta^2\phi_i'\phi_j' + 2\hat{N}\beta^2\phi_i''\phi_j'')\,\mathrm{d}X, \\
B(i,j) &= \int_0^1 (2\phi_i'\phi_j' + 2\beta^2\phi_i''\phi_j'')\,\mathrm{d}X.
\end{aligned}
$$

3. Numerical results and discussion

The boundary characteristic orthogonal polynomials as shape functions have been implemented in the Rayleigh–Ritz method to analyze vibration and buckling of single-walled carbon nanotubes embedded in an elastic medium (Fig. 1) under the influence of temperature. The elastic medium is modeled as Winkler-type and Pasternak-type foundations. The present formulation is based on the nonlocal Euler–Bernoulli beam theory. The effective properties of SWCNTs are taken as follows:[29,33] Young's modulus $E = 1000$ GPa, Poisson's ratio $\nu = 0.19$, $\alpha_x = -1.6 \times 10^{-6}$ for room temperature, and $\alpha_x = 1.1 \times 10^{-6}$ for high temperature. A computer code has been developed by the authors in MATLAB based on Eqs. (16) and (17).

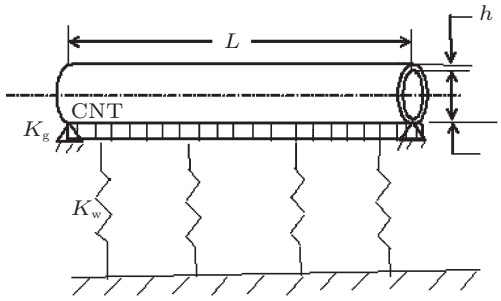


Fig. 1. Single-walled carbon nanotubes embedded within an elastic medium characterized by spring constant K_{w} and shear constant K_{g}.

3.1. Convergence

First of all, the convergence pattern has been carried out to compute results. Table 1 shows the convergence of the first three frequency parameters ($\sqrt{\lambda}$) of EBT nanobeams with CC support in a low temperature environment. In this table, we have taken $K_{\mathrm{w}} = 50$, $K_{\mathrm{g}} = 2$, $\theta = 20$ K, $e_0a = 0.5$ nm, and $L/d = 10$. Next, we show the convergence pattern graphically for buckling analysis. Figure 2 illustrates the convergence of critical buckling load parameter $\hat{P}_{\mathrm{cr}}$. In this figure, we have considered the CS edge condition with $L/d = 20$, $e_0a = 1$ nm, $K_{\mathrm{w}} = 60$, $K_{\mathrm{g}} = 4$, and $\theta = 10$ K. The above convergence patterns show that ten grid points are sufficient to obtain results in the present analysis.

Table 1. Convergence of the first three frequency parameters of CC nanobeams.

n	First	Second	Third
3	4.8718	7.8096	10.7781
4	4.8718	7.7285	10.7781
5	4.8718	7.7285	10.4761
6	4.8718	7.7273	10.4761
7	4.8718	7.7273	10.4657
8	4.8718	7.7273	10.4657
9	4.8718	7.7273	10.4656
10	4.8718	7.7273	10.4656
11	4.8718	7.7273	10.4656

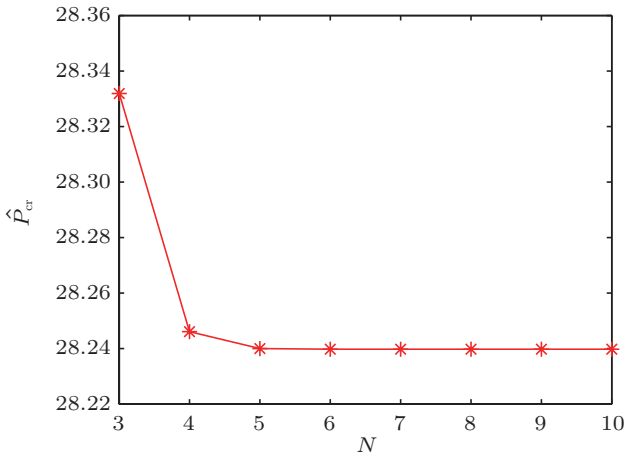


Fig. 2. (color online) Convergence of critical buckling load parameter.

3.2. Validation

To validate the present results, a comparison study has been carried out with the results of Wang *et al.*[21,22] In their analyses, the frequency and critical buckling load parameters have been given for four sets of boundary conditions. For this comparison, we have taken $K_{\mathrm{w}} = 0$, $K_{\mathrm{g}} = 0$, and $\theta = 0$ K. Figures 3 and 4 show the comparison for vibration and buckling analyses, respectively. We have considered SS support with $L/d = 10$ in Fig. 3 and CS support with $L/d = 14$ in Fig. 4. Excellent agreement in results is noticed from Figs. 3 and 4. Tabular comparison is shown in Table 22 for cantilever Euler–Bernoulli nanobeams with Ref. [45]. One may observe close agreement of the results with Ref. [45]. This shows the suitability and reliability of the present method for the vibration and buckling analyses of SWCNTs.

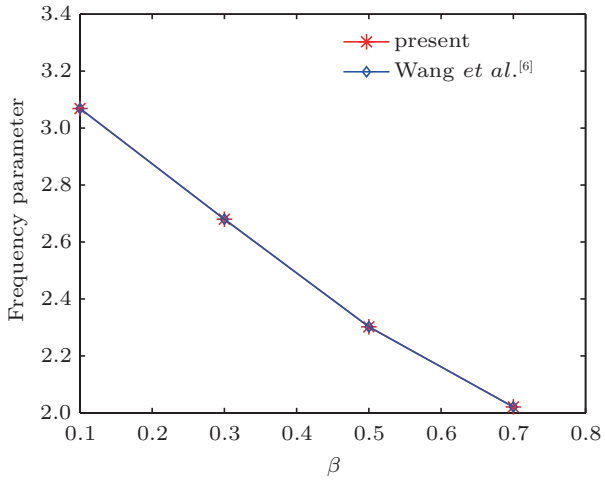


Fig. 3. (color online) Comparison of fundamental frequency parameter.

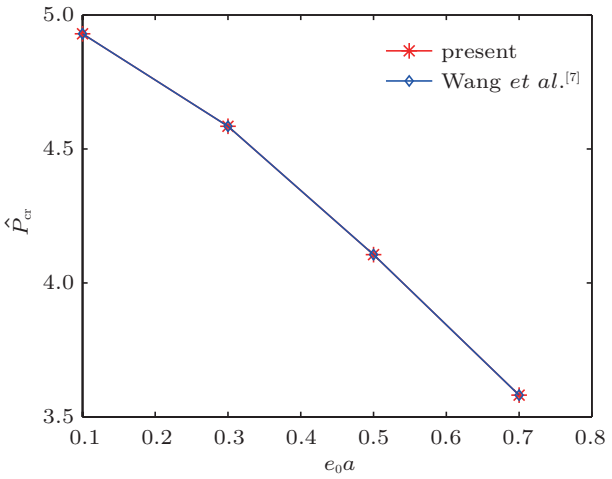


Fig. 4. (color online) Comparison of critical buckling load parameter.

Table 2. Comparison of cantilever Euler–Bernoulli nanobeams.

Preset	Ref. [45]	Present	Ref. [45]
29.235	29.444	29.235	29.444
180.12	180.80	171.25	171.89
485.02	485.10	423.56	423.99

3.3. Effect of Winkler modulus parameter

In this subsection, we investigate the influence of the surrounding medium on the vibration and buckling analyses of SWCNTs. The elastic medium is modeled as Winkler-type and Pasternak-type foundations. To show the effect of the Winkler modulus parameter, we consider EBT nanobeams with CS support in a low temperature environment. The various parameters are taken as $L/d = 10$, $K_g = 0$, $\theta = 20$ K. Figure 5 shows the effect of the Winkler modulus on the fundamental frequency parameter. In this figure, the results are shown for various scale coefficients ($e_0a = 0$ nm, 0.5 nm, 1 nm, 1.5 nm, 2 nm). The Winkler modulus parameter is taken in the range of 0–400. It is observed from this figure that the frequency parameter decreases with the increase in the scale coefficient. It may be noted that the results associated with $e_0a = 0$ nm correspond to those of the local beam theory. As the scale coefficient e_0a increases, the frequency parameter obtained from the nonlocal beam theory becomes smaller than that from its local counterpart. This is due to the fact that the nonlocal model may be viewed as atoms linked by elastic springs, while the local continuum model assumes the spring constant to take on an infinite value and the small scale effect makes the CNTs more flexible.[21] Therefore, the nonlocal theory should be considered for static and dynamic analyses of structures at nanoscale. It is also seen that the frequency parameter increases with the increase in the Winkler modulus parameter. This is because the nanotube becomes stiffer when the elastic medium constant is increased. This increasing trend of the fundamental frequency parameter with the surrounding elastic medium is influenced significantly by the small scale coefficients. Similarly, to analyze the effect of the Winkler modulus parameter on the buckling solutions, we take EBT nanobeams with CF support in a low temperature environment. The parameters are $K_g = 0$, $\theta = 30$ K, $L/d = 10$. Figure 6 shows the variation of the critical buckling load parameter with the Winkler modulus parameter. The scale coefficients are taken as $e_0a = 0$ nm, 0.5 nm, 1 nm, 1.5 nm, 2 nm. Here, the Winkler modulus parameter is also taken in the range of 0–400. It is seen that the critical buckling load increases with the increase in the Winkler modulus parameter. The cause may be that increasing the elastic medium constant makes the nanotube stiffer.[33] The buckling solutions are also affected by the small scale coefficients. The critical buckling loads are higher for lower scale coefficients. In addition, it is also observed that the critical buckling loads show a nonlinear behavior with respect to the stiffness of the surrounding matrix for higher e_0a. This may be due to the fact that the increase of the Winkler modulus causes CNT to be more rigid.

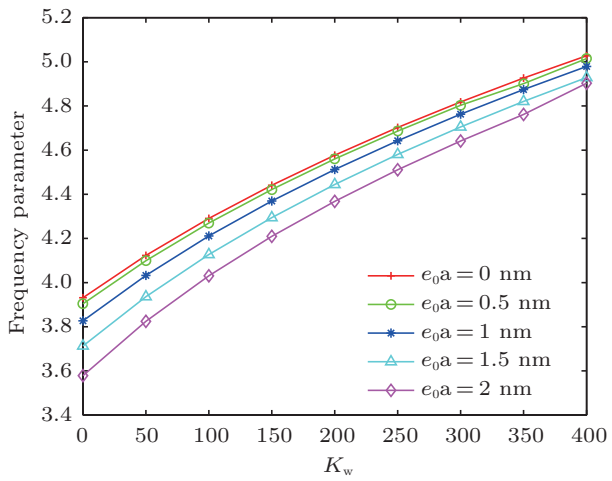


Fig. 5. (color online) Effect of the Winkler modulus parameter on the frequency parameter for various small-scale coefficients.

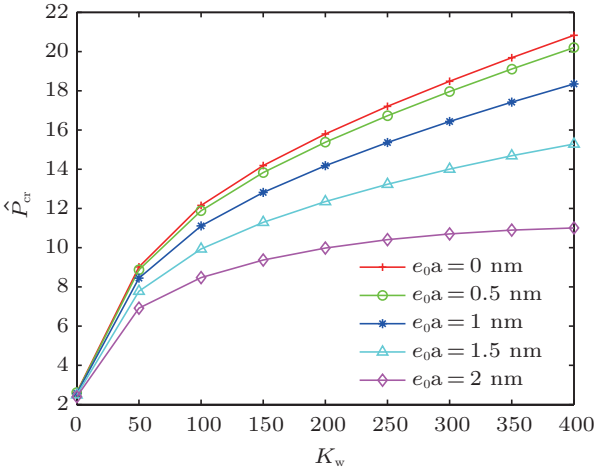


Fig. 6. (color online) Effect of the Winkler modulus parameter on the critical buckling load parameter for various small-scale coefficients.

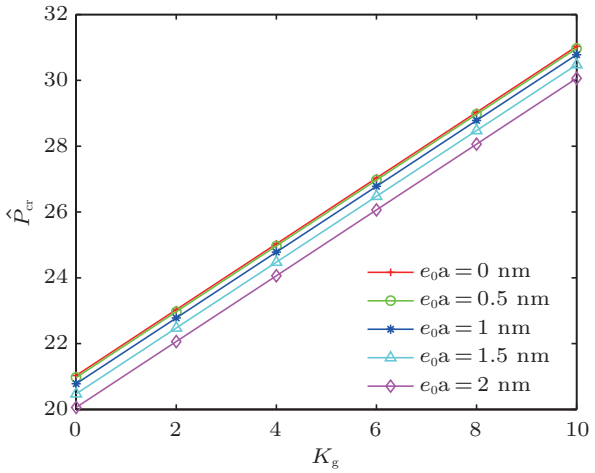


Fig. 8. (color online) Effect of the shear modulus parameter on critical buckling load parameter for various small-scale coefficients.

3.4. Effect of Pasternak shear modulus parameter

In this subsection, the effect of the Pasternak shear modulus parameter on the vibration and buckling solutions is examined. Figure 7 illustrates the fundamental frequency parameter as a function of the Pasternak shear modulus parameter K_g based on EBT with CC support in a low temperature environment. The parameters are $K_w = 0$, $L/d = 30$, and $\theta = 20$ K. The figure is plotted for various scale coefficients with the Pasternak shear modulus parameter ranging from 0 to 10. It is observed from the figure that the frequency parameter associated with the first mode increases with the Pasternak shear modulus parameter. This may be due to the effective stiffness of the elastic medium. With increase in the scale coefficient, the frequency parameter for a particular Pasternak shear modulus parameter decreases. Similarly, figure 8 shows the distribution of the critical buckling load parameter against the Pasternak shear modulus in a low temperature environment. The results are given for the EBT nanobeam with CS support.

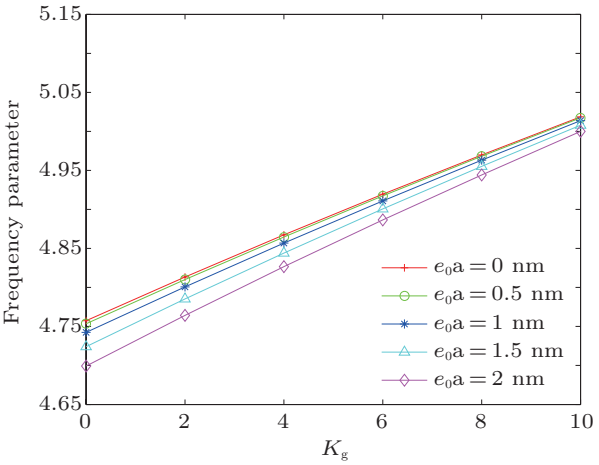


Fig. 7. (color online) Effect of the shear modulus parameter on frequency parameter for various small-scale coefficients.

The parameters are chosen as $K_w = 0$, $\theta = 10$ K, $L/d = 40$. Here, we have also incorporated the results for different scale coefficients. One may observe the same trend as that in the case of vibration. It is also observed that unlike the Winkler foundation model, the increase of the fundamental frequency parameter and the critical buckling load parameter with the Pasternak foundation is linear in nature. This is due to the domination of the elastic medium modeled as the Pasternak type foundation model. The same observation has also been reported in Ref. [33].

3.5. Effect of temperature

The effect of temperature on the vibration of nanobeams embedded in an elastic medium is investigated and shown in Fig. 9. In this graph, we have taken $L/d = 10$, $e_0a = 1.5$ nm, $K_w = 10$, $K_g = 4$. The results are shown for the EBT nanobeams with SS support in both high and low temperature environments. It may be seen that the frequency parameter varies linearly with the temperature change. Similarly, the effect of temperature on the buckling solutions is illustrated in Fig. 10. In this figure, we have taken SS nanobeams with $L/d = 20$, $e_0a = 2$ nm, $K_w = 50$, $K_g = 2$. It is noticed that the frequency and the critical buckling load parameters increase with increase in temperature in a low temperature environment while they decrease with increase in temperature in a high temperature environment. In a high temperature environment, the increase in temperature decreases the stiffness of the nanobeams and hence leads to lower frequency and critical buckling load parameters. Similarly, in a low temperature environment, the increase in temperature increases the stiffness of the nanobeams and hence leads to increased frequency and critical buckling load parameters. Thus, one may say that the frequency and critical buckling load parameters considering the thermal effect are larger than those ignoring the influence of the temperature change in a low temperature environment. Meanwhile, in a high temperature environment, the frequency

and buckling load parameters considering the thermal effect are smaller than those excluding the influence of the temperature change. The same observation has also been reported in Refs. [27], [28], [32], and [36].

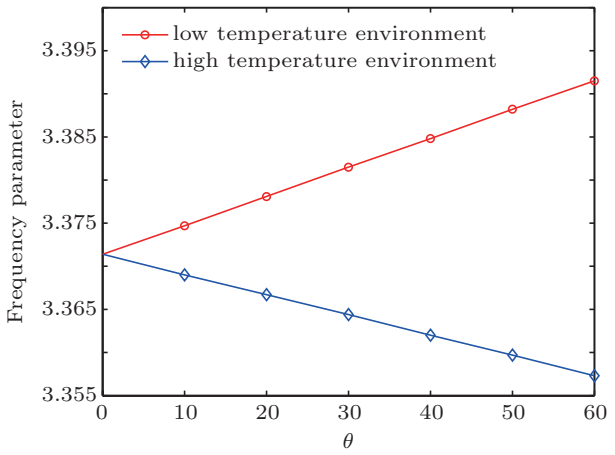


Fig. 9. (color online) Change of the frequency parameter with temperature in both low and high temperature environments.

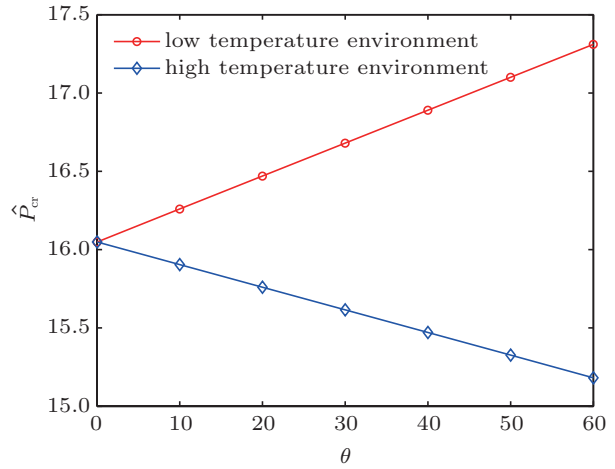


Fig. 10. (color online) Change of the critical buckling load parameter with temperature in both low and high temperature environments.

3.6. Effect of aspect ratio

To illustrate the effect of the aspect ratio on the fundamental frequency parameter, the variation of the scale load ratio (χ_{scale}) with the aspect ratio (L/d) is shown in Fig. 11 for different temperature changes. It may be noted that the scale load ratio is defined as χ_{scale} = frequency parameter calculated using nonlocal theory/frequency parameter calculated using local theory. It is observed that scale load ratio increases with increase in the aspect ratio. In addition, it is also seen that the frequency parameter is also dependent on the temperature change θ. The differences in the frequency parameter for different temperature changes are larger at low aspect ratios, while they are smaller at large aspect ratios. It is also seen that for larger temperature changes, the rate of the increase of the scale load ratio is smaller compared to that for smaller temperature changes. It may be noted that the same trend is also seen in the case of buckling.

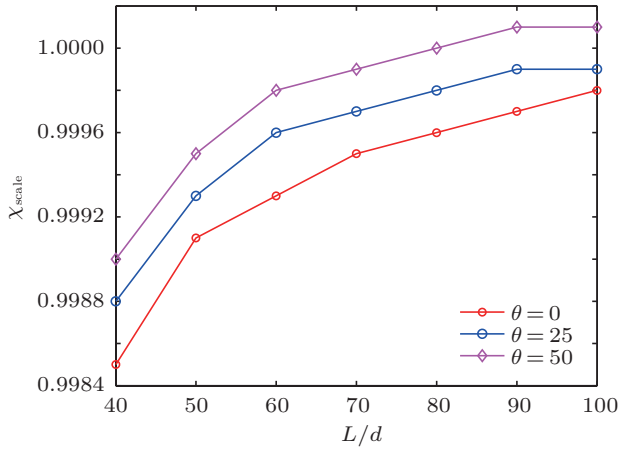


Fig. 11. (color online) Change of the scale-based frequency ratio with aspect ratio for different changes in temperature.

4. Conclusion

Boundary characteristic orthogonal polynomials as shape functions have been applied in the Rayleigh–Ritz method to investigate the thermal effect on the vibration and buckling of nanobeams embedded in an elastic medium. Four sets of boundary conditions have been taken into consideration. Theoretical formulations include effects of small scale, elastic medium, and temperature change. It is noted that the use of boundary characteristic orthogonal polynomials in the R–R method requires less computational effort because of the orthogonal property. It is seen that the results obtained based on the local beam theory are overestimated. The frequency and critical buckling load parameters increase with increase in temperature, Winkler type foundation, and Pasternak type foundation. It is also observed in the case of room or low temperature, the results obtained including the thermal effect are larger than those ignoring the influence of temperature, whereas in the case of high temperature, the results obtained with the thermal effect are smaller than those excluding the thermal effect.

References

[1] Tan Y and Wang Y G 2013 *Chin. Phys. Lett.* **30** 117901
[2] Tan Y and Wang Y G 2013 *Chin. Phys. Lett.* **30** 047901
[3] Tan Y and Wang Y G 2013 *Chin. Phys. Lett.* **30** 017902
[4] Tan Y and Wang Y G 2013 *Chin. Phys. Lett.* **30** 017901
[5] Wang W H, Wang W Z and Xu H X 2011 *Chin. Phys. Lett.* **28** 078103
[6] Jia W L, Zhao L, Hou L, Ji W L, Shi W and Qu G H 2014 *Acta Phys. Sin.* **63** 077201 (in Chinese)
[7] Wang Y L, Su K H, Yan H X and Wang X 2014 *Acta Phys. Sin.* **63** 046101 (in Chinese)
[8] Lei D, Menggen Q Q G, Zhang H L and Zhi Y B 2013 *Acta Phys. Sin.* **62** 248502 (in Chinese)
[9] Li M Y, Yu M, Su Q, Liu X Q, Xie E Q and Zhang X Q 2012 *Acta Phys. Sin.* **61** 236101 (in Chinese)
[10] Wang Y L, Su K H, Wang X and Liu Y 2011 *Acta Phys. Sin.* **60** 098111 (in Chinese)

[11] Shao Z F, Yang Y Q, Liu S T and Wang Q 2014 *Chin. Phys. B* **23** 096105
[12] Shao Z F, Yang Y Q, Liu S T and Wang Q 2014 *Chin. Phys. B* **23** 096102
[13] He C X, Jian Y, Qi X Y and Xue J K 2014 *Chin. Phys. B* **23** 025202
[14] Han Z D, Li X Y, Yang Z, Liu R P, Liu S D and Zhang Y 2012 *Chin. Phys. B* **21** 118102
[15] Ren Y, Ma W J, Zeng Q S, Li J Z, Dong H B and Zhou We Y 2012 *Chin. Phys. B* **21** 098103
[16] Iijima S 1991 *Nature* **354** 56
[17] Ruud J A, Jervis T R and Spaepan F 1994 *J. Appl. Phys.* **75** 4969
[18] Eringen A C 1972 *International Journal of Engineering Science* **10** 1
[19] Peddieson J, Buchanan G R and McNitt R P 2003 *International Journal of Engineering Science* **41** 305
[20] Xu M 2006 *Proceedings of the Royal Society A: Mathematical, Physical and Engineering Science* **462** 2977
[21] Wang C M, Zhang Y Y and He X Q 2007 *Nanotechnology* **18** 105401
[22] Wang C, Zhang Y, Ramesh S S and Kitipornchai S 2006 *J. Phys. D: Appl. Phys.* **39** 3904
[23] Reddy J 2007 *International Journal of Engineering Science* **45** 288
[24] Aydogdu M 2009 *Physica E* **41** 1651
[25] Ghannadpour S, Mohammadi B and Fazilati J 2013 *Composite Structures* **96** 584
[26] Ansari R, Sahmani S and Rouhi H 2011 *a Phys. Lett. A* **375** 1255
[27] Maachou M, Zidour M, Baghdadi H, Ziane N and Tounsi A 2011 *Solid State Commun.* **151** 1467
[28] Zidour M, Benrahou K H, Semmah A, Naceri M, Belhadj H A, Bakhti K and Tounsi A 2012 *Computational Materials Science* **51** 252
[29] Benzair A, Tounsi A, Besseghier A, Heireche H, Moulay N and Boumia L 2008 *J. Phys. D: Appl. Phys.* **41** 225404
[30] Wang L, Ni Q, Li M and Qian Q 2008 *Physica E* **40** 3179
[31] Zhang Y, Liu X and Liu G 2007 *Nanotechnology* **18** 445701
[32] Murmu T and Pradhan S 2009 *Computational Materials Science* **46** 854
[33] Murmu T and Pradhan S 2009 *Physica E* **41** 1232
[34] Narendar S and Gopalakrishnan S 2011 *Physica E* **43** 1185
[35] Ansari R, Gholami R and Darabi M 2011 *Journal of Thermal Stresses* **34** 1271
[36] Murmu T and Pradhan S 2010 *Computational Materials Science* **47** 721
[37] Tounsi A, Semmah A and Bousahla A A 2013 *Journal of Nanomechanics and Micromechanics* **3** 37
[38] Bhat R 1991 *Journal of Sound and Vibration* **149** 170
[39] Singh B and Chakraverty S 1992 *Journal of Sound and Vibration* **152** 149
[40] Singh B and Chakraverty S 1994 *Communications in Numerical Methods in Engineering* **10** 1027
[41] Singh B and Chakraverty S 1994 *Journal of Sound and Vibration* **173** 157
[42] Singh B and Chakraverty S 1994 *c Journal of Sound and Vibration* **173** 289
[43] Behera L and Chakraverty S 2014 *Meccanica* **49** 51
[44] Amirian B, Hosseini-Ara R and Moosavi H 2012 *Archives of Mechanics* **64** 581
[45] Li M and Zheng H 2013 *Research Journal of Applied Sciences Engineering and Technology* **5** 2729